Available online at www.sciencedirect.com

ScienceDirect

journal homepage: www.elsevier.com/locate/he

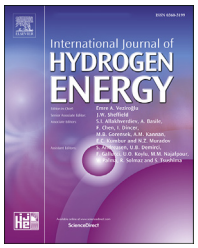

Dissecting the exergy balance of a hydrogen liquefier: Analysis of a scaled-up claude hydrogen liquefier with mixed refrigerant pre-cooling

David Berstad [a,*], *Geir Skaugen* [a], *Øivind Wilhelmsen* [a,b]

[a] *SINTEF Energy Research, Sem Sælands Vei 11, NO-7034, Trondheim, Norway*
[b] *NTNU, Department of Energy and Process Engineering, Kolbjørn Hejes Vei 1B, NO-7491, Trondheim, Norway*

HIGHLIGHTS

- Exergy analysis of a Claude hydrogen liquefier with mixed-refrigerant pre-cooling.
- Irreversibilities in all process components are calculated.
- The sum of exergy losses and useful output balances exactly with exergy input.
- The performance of simplified and detailed heat exchanger models are compared.
- Rational means for further process improvement are discussed.

ARTICLE INFO

Article history:
Received 5 July 2020
Received in revised form
6 September 2020
Accepted 23 September 2020
Available online 22 October 2020

Keywords:
LH_2
Liquid
Hydrogen
Liquefaction
Exergy
Irreversibility

ABSTRACT

For liquid hydrogen (LH_2) to become an energy carrier in energy commodity markets at scales comparable to for instance LNG, liquefier capacities must be scaled up several orders of magnitude. While state-of-the-art liquefiers can provide specific power requirements down to 10 kWh/kg, a long-term target for scaled-up liquefier trains is 6 kWh/kg. High capacity will shift the cost weighting more towards operational expenditures, which motivates for measures to improve the efficiency. Detailed exergy analysis is the best means for gaining a clear understanding of all losses occurring in the liquefaction process. This work analyses in detail a hydrogen liquefier that is likely to be realisable without intermediate demonstration phases, and all irreversibilities are decomposed to the component level. The overall aim is to identify the most promising routes for improving the process. The overall power requirement is found to be 7.09 kWh/kg, with stand-alone exergy efficiencies of the mixed-refrigerant pre-cooling cycle and the cryogenic hydrogen Claude cycle of 42.5% and 38.4%, respectively. About 90% of the irreversibilities are attributed to the Claude cycle while the remainder is caused by pre-cooling to 114 K. For a component group subdivision, the main contributions to irreversibilities are hydrogen compression and intercooling (39%), cryogenic heat exchangers (21%), hydrogen turbine brakes (15%) and hydrogen turbines (13%). Efficiency improvement measures become increasingly attractive with scale in general, and several options exist. An effective modification is to recover shaft power from the cryogenic turbines. 80% shaft-to-shaft power recovery will reduce the power requirement to 6.57 kWh/kg. Another potent modification is to replace the single mixed refrigerant pre-cooling cycle with a more advanced mixed-refrigerant cascade cycle. For substantial scaling-up in the long term, promising solutions can be

* *Corresponding author.*
E-mail address: david.berstad@sintef.no (D. Berstad).
https://doi.org/10.1016/j.ijhydene.2020.09.188

cryogenic refrigeration cycles with refrigerant mixtures of helium/neon/hydrogen, enabling the use of efficient and well scalable centrifugal compressors.

Background and motivation

The supply and distribution of liquid hydrogen (LH_2) has so far been catering only to a limited number of end-user categories, for instance aero-space and electronics/semiconductor industries [1]. Liquid-hydrogen distribution and use is also motivated by transport and distribution economics, since LH_2 trucks can transport several times more hydrogen per trip than compressed-hydrogen trucks. The near future will likely see new emerging users of LH_2 such as maritime transport [2]. Due to the limited global demand, the number of liquefiers and the capacities thereof have thus far been very limited. The current aggregate global hydrogen liquefaction capacity is reported to be around 355 ton per day (t_{LH2}/d) [3]. The single-train capacities are commonly in the range 5–15 t_{LH2}/d. Compared to liquefied natural gas (LNG), this is by all measures several orders of magnitude lower than full-scale liquefaction plants, with single-train capacities in the magnitude 10 000–20 000 ton LNG per day [4]. Although the use of hydrogen is already widespread in several global industries, with a total demand of 70 Mt/a high-purity hydrogen and 45 Mt/a crude hydrogen [5], it has the potential to become an even more important energy carrier in the future. The worldwide inequality of energy sources requires global trade and transport on a massive scale. In a future market for clean energy, the uneven distribution will largely remain prevalent. Hence, for hydrogen to become a true global energy commodity, the successful realisation of large-scale hydrogen transport is essential. Liquid hydrogen is an important candidate in this regard, provided a successful development and scaling-up of the LH_2 carrier technology to volumes similar to present-day LNG transport [6].

The potential penetration of LH_2 into other hydrogen markets and energy commodity markets will require capacities of substantially higher orders of magnitude, as well as lower power requirement for liquefaction. Hydrogen Claude cycles pre-cooled by externally supplied liquid nitrogen has been an ordinary technology for several decades and has seen a gradual reduction in power requirement as the development of crucial technology elements has progressed. During the last few decades the specific power requirement has evolved from typically 13.6 kWh/kg [7] to currently down to around 10 kWh/kg_{LH2} [8]. Looking forward, a specific power requirement of near 6 kWh/kg is a definite and plausible target for scaled-up liquefiers without the need for novel technologies [8]. This corresponds to an exergy efficiency of roughly 45%, depending on the exact feed and product condition. As a reference to realised industrial full-scale exergy efficiency, an advanced full-scale natural gas liquefier can have a specific power requirement of 0.23 kWh/kg_{LNG} [9] and thus an exergy efficiency as high as 48% when considering the ratio between the minimum reversible power requirement and the actual power input of the liquefaction plant.

In addition to scaling up current hydrogen liquefaction technology in the short-to mid-term, radically new technologies may also provide long-term options. Valenti and Macchi [10] proposed a liquefier concept with a capacity of 864 t/d, based on recuperative helium reverse Brayton cycles. With a feed pressure of 60 bar, the targeted power requirement and exergy efficiency were 5.04 kWh/kg and 47.7%, respectively. The study by Valenti and Macchi used considerably higher compressor and expander efficiencies compared to the present work, and also assumed the use of 15 inter-cooled axial, aeroderivative helium compressors. Each compressor was assumed to consist of eight stages so that the total number of compressor stages was 120. The results included a detailed exergy and loss categorisation. The IDEALHY project [11] proposed a hydrogen liquefier concept based on mixed-refrigerant pre-cooling and a helium/neon-based cryogenic refrigerant mixture in order to increase the average molecular weight beyond that of pure helium to around 8 kg/kmol, thus allowing a higher pressure ratio in the centrifugal compressors. The overall power requirement was estimated to around 6.4 kWh/kg [12]. Berstad et al. [13] investigated the use of a nine-component Kleemenko/auto-cascade pre-cooling cycle in a modified version of a liquefier concept first proposed by Quack [14], with a reverse Brayton cycle with a helium/neon refrigerant mixture. Specific power requirements were estimated to be in the range 6.2–6.5 kWh/kg.

With regard to previous studies on novel process concepts, Cardella et al. [15] pointed out issues related to the technical readiness and limitation of components, as well as the lack of cost focus. The development of new processes is, in other words, not a "race to the bottom" in power requirement, but about identifying rational and economically viable means for improving efficiency.

High capacity will shift the cost weighting more towards operational expenditures, hereunder energy cost, while the impact of capital expenditures decreases due to the inherent cost-scaling exponent of central pieces of equipment. This motivates for, and necessitates, more advanced and integrated process designs which can reduce parasitic thermodynamic losses and such reduce the specific power requirement. On the path towards large-scale, high-efficiency hydrogen liquefiers, it is of utmost importance to understand where and how these thermodynamic losses occur and how to rationally reduce them, that is, understand to what extent they can be reduced without overinvesting in efficiency-improving measures. The only means for achieving clear, unambiguous insights into the loss-drivers and the resulting

rational efficiency of a hydrogen liquefaction processes and its components and subsystems, is to apply exergy analysis.

There are numerous publications in the literature where different liquefier schemes are proposed, and in some cases subject to exergy analysis. Many of these, however, have fielded problematic design assumptions as well as partly incomplete or incorrect methodology for deriving the exergy balance. One recurring error is to ignore the chemical exergy terms whenever the chemical composition of a stream changes, which occurs for instance in mixed-refrigerant processes when streams are separated or mixed. This leads to incorrect results in exergy calculations for both separators and mixers. Refs. [16,17] are examples of works where this omission is made repeatedly. A consequence of this error is that irreversibilities are attributed to gravitational vapour–liquid separators in mixed-refrigerant pre-cooling cycles, even though the separators are assumed to be adiabatic, at phase equilibrium and without pressure losses or quantified changes in potential and kinetic exergy. With these assumptions, the irreversibility will amount to zero when the exergy balance is used correctly. The results become incorrect also for mixers since the chemical exergy terms are omitted. When the separator feed is made up of a single component in the two-phase region, the chemical exergy terms balance inevitably and can be eliminated in the exergy balance. Only in this case, by serendipity, is the separator irreversibility correctly calculated to zero by use of the thermo-mechanical exergy terms. This is the case in Ref. [18], in which the correct zero value was obtained using the incomplete expression for the separator exergy balance, adopted directly from Ref. [17], but applied to a single-component, two-phase hydrogen process stream. A questionable assumption used in several works [16–21] is to specify the pressure drop in all heat exchangers and compressor intercoolers to be zero. The results presented in this work show that irreversibilities caused by pressure losses in heat exchangers and intercoolers are by no means negligible.

In this work, the exergy balance and all irreversibilities of a scaled-up Claude hydrogen liquefier with mixed-refrigerant pre-cooling will be mapped. The useful exergy transfer and exergy losses in the process of liquefying feed hydrogen, as well as recompression and re-liquefaction of boiloff gas returning from the liquid hydrogen storage, will be broken down to the single-component level and attributed to different mechanisms such as heat transfer losses and pressure losses. To avoid errors in the analysis, a self-check of the exergy calculations will be carried out through a comparison of the aggregate results for bottom-up, unit-wise exergy conversion results with that of the net exergy input through compression power. No recovery of shaft power from cryogenic turbines is assumed, which is instead dissipated, but the resulting power requirement is still substantially lower than the specific power requirement of state-of-the-art liquefiers, which is around 10 kWh/kg with liquid nitrogen pre-cooling [8]. The process configuration, capacity and efficiency considered are generally in accordance with what the industry may provide without the need for demonstration phases [22]. It should be noted that mixed-refrigerant pre-cooling has not been deployed in industrial hydrogen liquefiers but is standard LNG technology, and has been tested by SINTEF Energy Research in a small laboratory-scale hydrogen liquefier [23]. The detailed exergy analysis constitutes an excellent basis to approach the overall aim of identifying the most promising routes to further improving the process. The usefulness of such a detailed overview and ranking of irreversibilities is considerable and reveals what impact the relative improvement of different components and sub-systems has on the overall liquefier efficiency and power requirement. When this quantitative information is combined with the know-how of process developers and vendors, improvement measures can be ranked and prioritised.

Liquefaction process description

Fig. 1 depicts the process flow diagram of the hydrogen liquefaction process in consideration. Hydrogen is fed to the liquefier at a rate of 125 t/d at 20 bar and 298.15 K. Limiting the feed pressure to around 20 bar is a rational choice provided that the hydrogen feed is expanded isenthalpically, or closely thereto, from around 30 K. This can be understood by considering the isenthalpic lines and the Joule–Thomson coefficient $(\partial T/\partial p)_h$ for different pressure levels at 30 K temperature. As described below, the hydrogen feed is expanded as the motive stream through an ejector. Since the ejector has a relatively low entrainment ratio, the isenthalpic approximation can still be used to justify the choice of feed pressure. Exceeding 20 bar pressure will lead to an increasingly negative Joule–Thomson coefficient and will be counterproductive as it will lead to an increasingly higher vapour-fraction and thus lower liquid yield. A potential benefit of compressing the hydrogen feed to a higher pressure is a more evenly distributed heat capacity and a slight net efficiency improvement if a dense-phase expander is added. However, economic optimisation has indicated that additional feed compression will not pay off [8].

In the heat exchangers HX-1 and HX-3 through HX-6, the hydrogen is cooled to 30 K. The first cooling stage is a single-stage, mixed-refrigerant cycle utilising a five-component refrigerant mixture (nitrogen, methane, ethane, propane and n-butane) to cool the hydrogen feed to 114 K in heat exchanger HX-1. Refrigerant compression to 35 bar is provided by two intercooled compressor stages. Each compressor is specified to have an isentropic efficiency of 85% and each intercooler is assumed to have a pressure drop of 20 kPa and a hot-side outlet temperature of 298.15 K. After the first intercooling stage the refrigerant condenses partially, and the liquid condensate is separated in a liquid receiver and pressurised to 35 bar with a condensate pump with 75% efficiency. In HX-1, the pressurised refrigerant is, like the hydrogen feed, cooled to 114 K and thereafter expanded isenthalpically to 3.6 bar, resulting in a temperature of 111.3 K, which is about 7 K above the estimated freeze-out temperature of the heaviest component in the refrigerant mixture. After expansion, the cold refrigerant returns through HX-1 in cold-side passes in the same heat exchanger, giving a tight thermal match and thus an exergy-efficient heat transfer between the two hot streams and the cold stream.

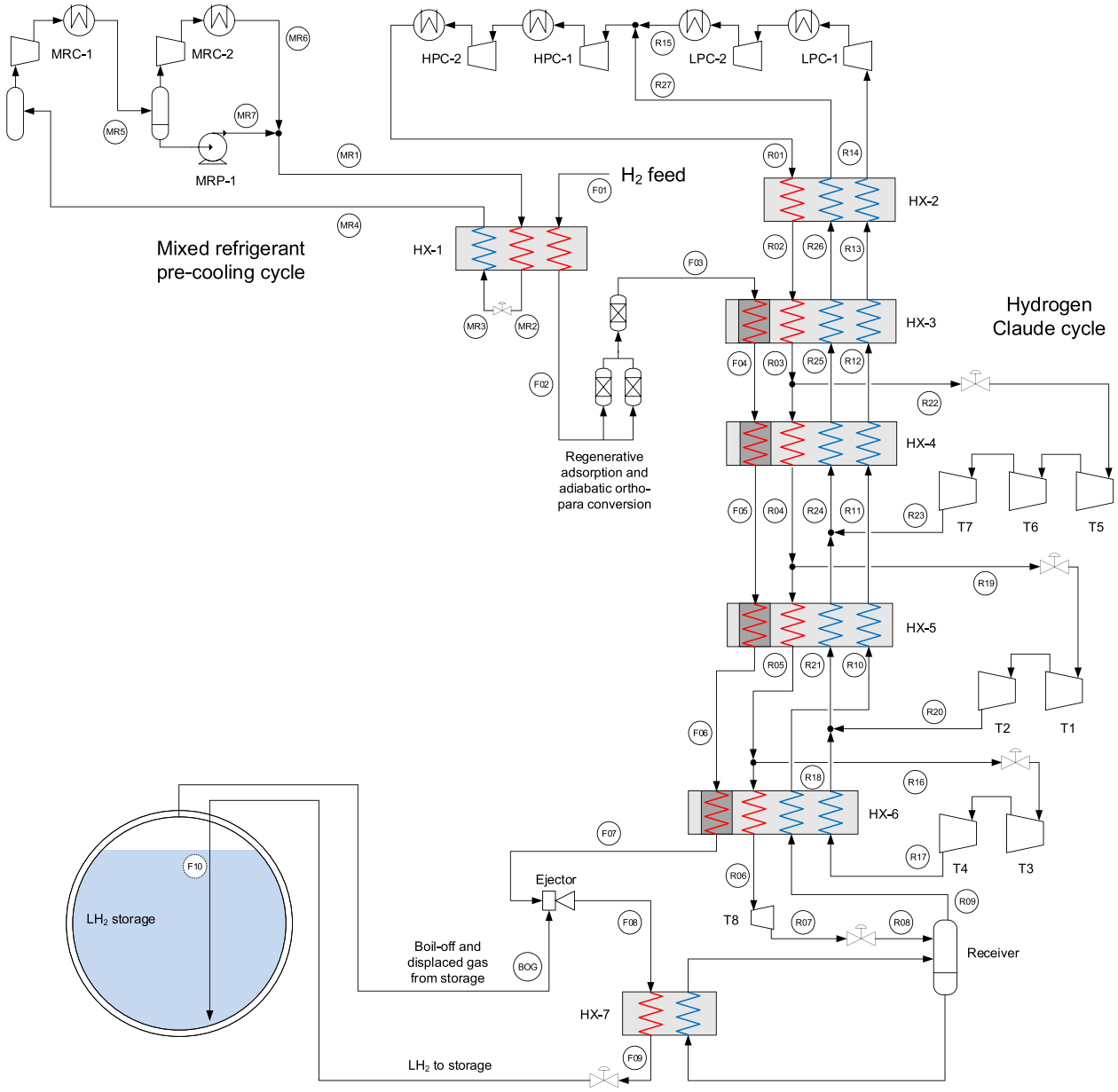

Fig. 1 – Hydrogen liquefier process flow diagram.

Fig. 2 shows the temperature difference between the composite curves in HX-1, including a comparison with the corresponding results by Cardella et al. [15]. The temperature difference is plotted as a function of the normalised heat transfer rate. The profiles are comparable across most of the scale, while the peak temperature difference towards the hot end of the heat exchanger, as well as the hot-end temperature difference, are higher in the present work. This implies that slightly lower heat transfer exergy losses and thus somewhat lower pre-cooling power demand can be obtained by making modest changes in refrigerant composition, pressure levels and flowrate. Fig. 2 also includes the cumulative irreversibility in HX-1 caused by finite-temperature heat transfer and pressure losses, respectively. The methodology basis for the exergy calculations is presented in a dedicated section below.

Before further cooling in HX-3, the hydrogen feed is assumed to be brought to an equilibrium composition between the two spin isomers ortho- and para-hydrogen. This is obtained by passing the gas through an adiabatic, fixed-bed reactor catalysing the spontaneous and exothermic conversion of ortho-hydrogen to para-hydrogen. It is assumed that the reactor is sufficiently long to allow the new equilibrium state to form. The outlet state is calculated to be 117.9 K, 19.8 bar with around 33.2 mol% para-hydrogen. From this state, the hydrogen feed is cooled to 30 K in heat exchangers HX-3 through HX-6, which are assumed to be catalyst-filled on

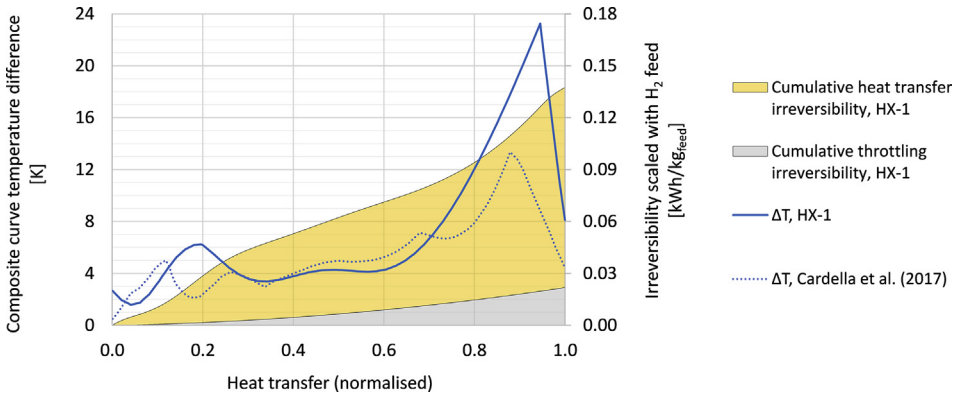

Fig. 2 – A comparison of the temperature difference between composite curves for HX-1 and optimised mixed-refrigerant pre-cooling process by Cardella et al. [15]. Also shown is the cumulative irreversibility caused by finite-temperature heat transfer and by pressure losses.

the feed-H_2 side. In these heat exchangers, the full refrigeration duty is provided by cold hydrogen gas generated by the hydrogen Claude cycle. In this refrigeration cycle, a high-pressure hydrogen stream is pre-cooled to 112 K in heat exchangers HX-2 and HX-3. From this node on and further down the high-pressure line, side streams are drawn from the main high-pressure line, expanded to an intermediate pressure level in cryogenic hydrogen turbines to induce temperature drops, and subsequently fed to an intermediate-pressure gas return line which provides the main cooling duty in all heat exchangers except of HX-1 and HX-7. Each cryogenic turbine is assumed to have an isentropic efficiency of 85%, a performance that has been verified on a 40 kW scale [24]. Each turbine pair or triplet has an upstream control valve with an assumed pressure drop of 12 kPa.

After cooling to 30 K, the hydrogen feed is expanded to 1.85 bar through an ejector. This stream also functions as the motive stream expanded in a nozzle to entrain and recompress boiloff gas from the liquid hydrogen storage. Boiloff gas arises from two different mechanisms with different causes. Firstly, heat ingress into the storage tank is assumed to cause a constant boiloff rate. Secondly, constant delivery from the liquefier causes accumulation of LH_2 and thus displacement of hydrogen vapour occupying the ullage space in the storage tank. With an assumed boiloff rate of 0.1% per day caused by heat ingress, the overall boiloff gas return rate to be recompressed by the ejector is 7.1 t/d, that is, 5.7% relative to the hydrogen feed stream of 125 t/d. This figure is commonly referred to as the entrainment ratio for ejectors. The ejector efficiency equals 2.4% according to the common definition [25].

A smaller fraction, of the high-pressure stream in the Claude cycle, 4.6% of the total mass flow, is expanded by a dense-phase expander and a throttling valve in series, to 1.33 bar. The resulting two-phase discharge stream is sent to a liquid receiver that is assumed to keep HX-7 flooded with liquid hydrogen on the cold side, which in turns ensures condensation and subcooling of the two-phase ejector discharge stream, which is made up of expanded hydrogen feed and recompressed boiloff gas from the liquid hydrogen storage. All the hydrogen that evaporates on the cold side of HX-7 and in the throttling valve at the receiver inlet, is sucked from the receiver tank by the low-pressure hydrogen compressors. This hydrogen stream passes through all heat exchangers in the Claude process before it is re-compressed in the low-pressure compression stages LPC-1 and LPC-2, mixed with the returning intermediate-pressure stream and further compressed to 30 bar in HPC-1 and HPC-2. The isentropic efficiencies of the low- and high-pressure hydrogen compressors stages are assumed to be 82% and 85%, respectively.

After subcooling in HX-7, the liquid hydrogen product is transferred from the liquefier to the storage, assumed to have a total volume of 50,000 m^3. The storage tank pressure is assumed to be 1.50 bar at the liquid interface. During transfer, the liquid hydrogen is transferred in a vacuum-insulated pipeline and ascends 45 m in a vertical riser outside the tank, and thereafter descends 45 m to the tank bottom through a downcomer on the inside. The fresh liquid hydrogen product is subcooled by a margin of 0.21 K at the interfacial storage tank pressure of 1.50 bar. The tank feed system can in principle be via such a downcomer, via spray injection from the top to de-superheat the vapour phase, or a combination of both. The LH_2 transfer and storage systems are not considered in further detail in this work, but the irreversibilities caused by the transfer between the liquefier and storage tank are accounted for. Principal stream data for the hydrogen feed, mixed-refrigerant cycle, and Claude cycle, are summarised in Table 1.

The process model was built in steady-state mode using the commercial process simulation tool Aspen HYSYS V9, using different Equations of State (EoS) depending on the fluid in consideration. Peng–Robinson was used to represent the thermodynamic properties of the mixed refrigerant while the modified Benedict–Webb–Rubin (MBWR) EoS was used for

Table 1 – Stream data. Stream numbering refers to Fig. 1.

Stream ID	Temp.	Pressure	Mass flowrate	Vapour fraction	Stream ID	Temp.	Pressure	Mass flowrate	Vapour fraction
	K	bar	kg/h	mol/mol		K	bar	kg/h	mol/mol
F01	298.15	20.000	5208	1	R13	114.28	1.317	2252	1
F02	114.00	19.910	5208	1	R14	296.08	1.297	2252	1
F03	117.92	19.810	5208	1	R15	298.15	7.477	2252	1
F04	106.00	19.758	5208	1	R16	47.40	28.853	16,142	1
F05	72.50	19.658	5208	1	R17	30.10	7.895	16,142	1
F06	46.00	19.508	5208	1	R18	43.95	7.863	16,142	1
F07	30.00	19.458	5208	0	R19	74.00	28.86	14,546	1
F08	22.49	1.850	5504	0.298	R20	47.16	7.863	14,546	1
F09	21.44	1.840	5504	0	R21	45.46	7.863	30,688	1
F10	21.47	1.500	5504	0	R22	112.00	29.04	16,200	1
BOG	21.68	1.500	295.7	1	R23	73.56	7.823	16,200	1
					R24	72.47	7.823	46,888	1
R01	298.15	29.800	49,141	1	R25	104.95	7.683	46,888	1
R02	119.45	29.620	49,141	1	R26	114.28	7.627	46,888	1
R03	112.00	29.040	49,141	1	R27	296.08	7.477	46,888	1
R04	74.00	28.860	32,941	1					
R05	47.40	28.853	18,394	1	MR1	300.10	35.000	72,000	0.645
R06	30.00	28.846	2252	0	MR2	114.00	34.790	72,000	0
R07	28.33	7.188	2252	0	MR3	111.32	3.600	72,000	0.069
R08	21.23	1.330	2252	0.225	MR4	291.99	3.190	72,000	1
R09	21.31	1.330	2252	1	MR5	298.15	12.066	72,000	0.902
R10	43.95	1.322	2252	1	MR6	298.15	35.000	60,704	0.744
R11	71.90	1.321	2252	1	MR7	299.92	35.000	11,296	0
R12	104.95	1.319	2252	1					

hydrogen. The MBWR EoS was verified to give very similar results as the multiparameter EoS by Leachman et al. [26], and was chosen because it was computationally more efficient. The steady-state representation of continuous ortho-para conversion at equilibrium was obtained by modifying the REFPROP [27] fluid file for hydrogen to represent "equilibrium-hydrogen" as suggested by Valenti et al. [28]. By adopting this hydrogen model, the present liquefier model assumes continuous equilibrium conversion through the heat exchangers HX-3 to HX-6. This means that we are using an ideal assumption, from which realities will diverge to a certain extent. We have recently shown in detail how longitudinal exergy losses [W/m] in cryogenic, catalyst-filled plate-fin and spiral-wound heat exchangers occur in hydrogen liquefiers, and how they are driven by the mechanisms finite-temperature heat transfer, pressure drop and lagging, off-equilibrium ortho-para conversion [29]. By comparing to these results, we shall for the first time evaluate the precision of the "equilibrium hydrogen" model. It can be expected that the actual para-hydrogen content will be somewhat lower than the equilibrium concentration after cooldown. If it is desirable to maximise the para-hydrogen content of the final LH_2 product in order to minimise boiloff induced by spontaneous conversion during subsequent storage, the condensing and subcooling heat exchanger HX-7 can also be filled with catalyst material to function as an additional conversion bed.

Methodology – calculation of exergy balance of system, sub-systems and components

The general exergy balance of an open control volume in steady state can be expressed as [30]:

$$\dot{I} = -\dot{W}_{shaft} + \sum_{in}\dot{m}_i\epsilon_i - \sum_{out}\dot{m}_e\epsilon_e + \sum_r \dot{Q}_r\left(1-\frac{T_0}{T_r}\right) \quad (1)$$

In this equation, $\dot{I}$ denotes the total irreversibility rate within the control volume boundaries, $\dot{W}_{shaft}$ is the overall shaft work directed out of the control volume, $\dot{Q}_r$ is the heat flowing into the control volume at temperature T_r, $\dot{m}$ is the mass flowrate of each material stream entering or leaving the control volume and ϵ is the accompanying specific exergy of each material stream. The mass flowrate $\dot{m}$ [kg/s] and specific exergy ϵ [kJ/kg] in Eq. (1) can alternatively be expressed on a molar basis with molar flowrate $\dot{N}$ [kmol/s] and molar exergy $\bar{\epsilon}$ [kJ/kmol]. The specific exergy in Eq. (1) is the sum of four terms:

- Kinetic exergy, ϵ_k
- Potential exergy, ϵ_p
- Thermo-mechanical exergy, ϵ_{tm}
- Chemical exergy, ϵ_{ch}

In all practical aspects of the following calculations, the changes in kinetic and potential exergy are assumed to be negligible in comparison to changes is thermo-mechanical and chemical exergy. Hence, the exergy balanced derived in the following sections will disregard the kinetic and potential exergy terms. It must be noted that this is not a valid assumption when considering the conversion of energy inside components such as turbo-compressors, cryo-expanders and ejectors, in which there are significant conversions between pressure-based enthalpy and kinetic energy. Since locally high velocities are reduced by impeller blades or diffusors before the fluid leaves the component in consideration, the

change in kinetic exergy can still be disregarded for the component as such.

The specific thermo-mechanical exergy for a fluid in an arbitrary thermodynamic state (*h*,*s*) is expressed as:

$$e_{tm} = h - h_0 - T_0(s - s_0) \quad (2)$$

where h_0 and s_0 is the respective specific enthalpy and entropy at ambient temperature T_0 and pressure p_0. The chemical exergy $\bar{e}_{ch}$ on a molar basis is expressed as:

$$\bar{e}_{ch} = \sum_j x_j \bar{e}_j^0 + \left(\bar{h}_0 - \sum_j x_j \bar{h}_{0,j} - T_0\left(\bar{s}_0 - \sum_j x_j \bar{s}_{0,j}\right)\right) \quad (3)$$

where x_j is the mol fraction of chemical component j, $\bar{e}_j^0$ is the standard chemical exergy of component j, $\bar{h}_0$ and $\bar{s}_0$ is the molar enthalpy and entropy at ambient temperature and pressure for the full composition, and $h_{0,j}$ and $s_{0,j}$ is the respective single-component molar enthalpy and entropy at ambient temperature and pressure.

From gaseous feed to liquefied hydrogen product – useful exergy output of the liquefier

The function of the liquefier is to bring the hydrogen feed to the target liquid state. The exergy added to the hydrogen during liquefaction is thus to be counted as the useful exergy output of the process. The exergy difference between the feedstock and the liquid product depends on several factors. The thermodynamic state of the high-purity hydrogen feed is largely a function of pressure and temperature, while that of the liquefied product depends additionally on the para-hydrogen content [31]. In addition, the ambient temperature has a significant impact on the exergy calculation. Berstad et al. [31] showed that the hydrogen feed pressure is by far the most sensitive parameter in this regard and provided illustrative examples showing that exergy efficiency for a given liquefaction process will change significantly with feed pressure. If feedstock compressors are included in the liquefier control volume, the overall exergy efficiency can be higher for a low-pressure feed than for a high-pressure feed, despite having a higher specific power requirement.

Fig. 3 shows the specific exergy difference, i.e. the minimum liquefaction work between product and feed at T_0 as a function of feed pressure and liquid-product pressure at the equilibrium para-hydrogen composition. In the calculations, we assumed saturated liquid as thermodynamic state in the product. The ambient temperature is assumed to be 288.15 K and this value is used in all exergy calculations. The graphs show that the feed pressure has a major impact on the minimum liquefaction work, i.e. the exergy difference between gaseous feed and liquid product. In comparison, the liquid-product pressure, given saturated liquid, has only a minor influence within the 1.3–1.7 bar interval plotted.

In the liquefaction process under consideration, the hydrogen feed is continuously converted in heat exchangers HX-3 through HX-6, where the outlet temperature is 30 K. At this point, the para-hydrogen fraction is assumed to be at equilibrium conditions, that is, close to 97%. This is assumed

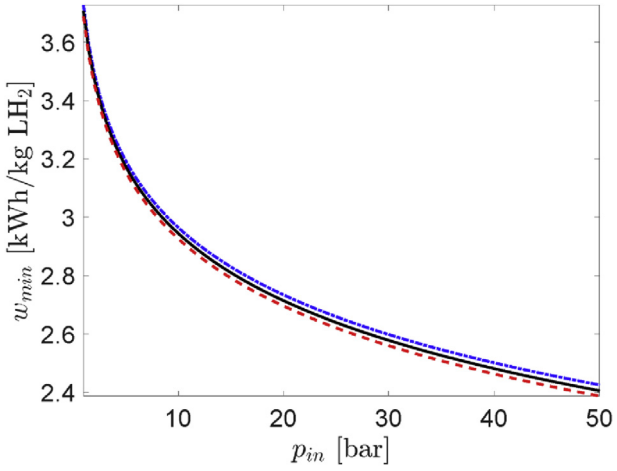

Fig. 3 – Minimum liquefaction work, w_{min}, for different inlet pressures, p_{in}, and three different choices of outlet pressures: 1.3 bar (blue dash-dot line), 1.5 bar (solid line), 1.7 bar (red dashed line). Obtained by computing the specific exergy difference between the feed hydrogen and the product hydrogen, which is assumed to be a saturated liquid hydrogen, where the para-hydrogen mole fraction has its equilibrium value at the saturation temperature. The hydrogen has been assumed to be an ideal mixture between ortho- and para-hydrogen described by the EoS by Leachman et al. [26]. (For interpretation of the references to color in this figure legend, the reader is referred to the Web version of this article.)

to be the final composition of the liquid hydrogen product. Hence, the minimum specific liquefaction work required to transform the 20-bar hydrogen feed to liquid hydrogen at 1.50 bar and 0.2 K subcooled state is estimated to 2.67 kWh/kg.

In addition to liquefaction of the hydrogen feed, recompression and re-liquefaction of boiloff gas from the hydrogen storage is also included in the liquefier process and in the calculation of mass balances and duties. Regarding the state of the boiloff gas, the following assumptions have been made: It is assumed that the thermodynamic state in the storage tank is aged hydrogen at equilibrium conditions at 1.50 bar. In a static LH_2 storage tank, there will usually be non-uniform temperature distribution in the liquid and vapour phases, but in large storage tanks for future, large-scale operation (volumes in the magnitude of 10^4 m^3) the gas can be de-superheated by ancillary spray-injection or bubbling systems if desirable. This implies that the returning boiloff stream is saturated vapour with 99.5% para-hydrogen fraction. The minimum specific liquefaction work required to re-liquefy saturated vapour with 99.5% para-hydrogen fraction at 1.50 bar to subcooled liquid at equal pressure level and approximately 0.2 K subcooling is estimated to 1.50 kWh/kg$_{BOG}$. Depending on the length and insulation standard of the vapour return line, the boiloff gas will inevitably be somewhat superheated, but the extent is more a design issue with respect to piping and ejector design. However, a vacuum-

insulated return line should keep the superheating level low [32].

Heat exchangers

For a generic, multi-stream heat exchanger with negligible heat exchange with its surroundings and negligible changes in kinetic and potential exergy, the exergy balance in Eqs. (1) and (2) reduces to:

$$\sum_j \dot{E}_{j,in} = \sum_j \dot{E}_{j,out} + \dot{I} \tag{4}$$

The total irreversibility rate can be expressed as:

$$\dot{I} = \sum_j \dot{m}_j \left(h_{j,in} - h_{j,out} - T_0\left(s_{j,in} - s_{j,out}\right)\right) \tag{5}$$

Black-box-based exergy balances such as that expressed in Eq. (5) apply to heat exchangers in steady state where the chemical composition remains unchanged for all streams. This is sufficient for quantifying the sum of all irreversibilities that occur in the control volume encompassing the heat exchanger. This figure does, however, not decompose and quantify the causes of irreversibility related to the impact of pressure losses and finite-temperature heat transfer, respectively.

The irreversibilities caused by pressure loss through a heat exchanger of length L with n layers is expressed as [33]:

$$\dot{I}_{\Delta p} = \int_0^L \left[\sum_{j=1}^n T_0 A_j v_j \left(-\frac{1}{T_j}\frac{dp_j}{dz}\right)\right] dz, \tag{6}$$

where A and v denote cross-section area and velocity, respectively. The present work assumes simpler, zero-dimension heat exchanger models where the total pressure drop per stream correlates linearly with duty. In this case, assuming a linear pressure drop in Eq. (6), the expression can be reduced in order to calculate $\dot{I}_{\Delta p}$:

$$\dot{I}_{\Delta p} = \sum_{j=1}^n \left[\dot{m}_j T_0 \int_{p_{in,j}}^{p_{out,j}} -\frac{1}{\rho_j T_j} dp_j\right] \tag{7}$$

In Eq. (7), n represents the number of streams and $\dot{m}_j$, p_j, ρ_j and T_j is the mass flowrate, pressure, density and temperature, respectively, of stream j.

An exception where the exergy balance in Eq. (5) does not apply, is when there are chemical exergy changes in the process stream, which in practice applies to the heat exchangers in the hydrogen liquefier in which catalysed, non-equilibrium ortho-para conversion takes place. For these non-equilibrium cases, the chemical exergy must be included, and the analysis must be extended into further detail.

Adiabatic ortho-para conversion

The pre-cooling heat exchanger, HX-1 does not have catalyst-filled channels on the feed-hydrogen side. There are mainly two reasons for this. Since the feed hydrogen contains a certain amount of trace purities, typically in the range of 10–100 ppm, a heat exchanger-internal catalyst bed would act as an adsorption bed in addition to catalysing ortho-para conversion and thus lose activity over time. Another reason is that the equilibrium composition of ortho- and para-hydrogen changes only moderately between ambient temperature and the pre-cooling temperature level, and introduction of catalyst in the pre-cooling section may cause excessive pressure drop and only small gains in para-hydrogen concentration. Due to the relatively high temperature level and correspondingly low conversion heat, the lag in ortho- and para-hydrogen composition causes only modest thermodynamic losses. In an adiabatic reactor for ortho-para conversion, the irreversibility rate density that comes from the entropy production is:

$$\dot{I}_{rx,T} = rT_0\left(\frac{-\Delta G_{\{rx,T\}}}{T}\right), \tag{8}$$

where subscript rx refers to reaction, subscript T refers to the temperature, r is the reaction rate and $\Delta G_{\{rx,T\}}$ is the Gibbs energy of the ortho-para hydrogen conversion at temperature T.

Mixing of streams with different composition or thermodynamic state

There are several examples of splitting and mixing of process streams in the hydrogen liquefaction process. Splitting or separation of single- or two-phase streams in thermodynamic equilibrium can be done reversibly without causing irreversibilities. Mixing single- or two-phase streams in different thermodynamic states that are not in thermodynamic equilibrium with the state of the resulting mixture, will lead to irreversibilities.

Mixing of single-component, gaseous hydrogen gas streams with different thermodynamic state

In the hydrogen Claude cycle, there are several mixing points where two normal-hydrogen streams are mixed. These have slightly differing temperatures, while the pressure levels are assumed to be equal. For the mixing of two single-component gaseous streams 1 and 2 into a product stream 3, and assuming adiabatic operation, Eqs. (1) and (2) reduce to:

$$\dot{I} = \dot{m}_1(h_1 - T_0 s_1) + \dot{m}_2(h_2 - T_0 s_2) - \left(\dot{m}_1 + \dot{m}_2\right)(h_3 - T_0 s_3) \tag{9}$$

The first law of thermodynamics can be used to obtain the explicit expression for h_3:

$$h_3 = h_1\frac{\dot{m}_1}{\dot{m}_1 + \dot{m}_2} + h_2\frac{\dot{m}_2}{\dot{m}_1 + \dot{m}_2} \tag{10}$$

The outlet entropy s_3 is a function of the two thermodynamic properties h_3 and p_3.

Mixing of multicomponent refrigerant streams with different composition and thermodynamic state

The mixed refrigerant consists of five components of highly different volatilities. Intercooling this mixture between the first and second compression stage leads to condensation of a significant fraction of the refrigerant, dominated by the heaviest components. Hence, a liquid receiver and demister

must separate the vapour from the liquid before the second compressor. The near-incompressible liquid can be pumped to higher pressure with very low energy demand. After the second gas compression and aftercooler stage, further condensation of predominantly heavier components will occur. The two-phase Stream 1 and the subcooled liquid Stream 2 discharged from the pump are assumed to be mixed forming Stream 3, which causes irreversibilities and resumption to the previous chemical composition, but at a new thermodynamic equilibrium and phase distribution. The irreversibility for the mixing process can be calculated by combining Eqs. (1)–(3):

$$\dot{I} = \dot{N}_3\left(\overline{\varepsilon}_{tm,3} + \overline{\varepsilon}_{ch,3}\right) - \left[\dot{N}_1\left(\overline{\varepsilon}_{tm,1} + \overline{\varepsilon}_{ch,1}\right) + \dot{N}_2\left(\overline{\varepsilon}_{tm,2} + \overline{\varepsilon}_{ch,2}\right)\right] \quad (11)$$

Values for the standard chemical exergy used in calculations are adopted from Ref. [30].

Compressors and intercoolers

Six compressors and inter-/aftercoolers are present in the liquefaction process. For the heavier mixed-refrigerant composition, two centrifugal compressors are assumed while the hydrogen gas is assumed to be compressed by four single-stage oil-free piston compressors. Although the two different compressor types, impulse and displacement, are fundamentally different, a generic representation and control volume of a compressor–cooler pair, as illustrated in Fig. 4, can be used to derive the exergy balance.

Assuming adiabatic compression and neglecting changes in kinetic and potential exergy, Eqs. (1) and (2) applied to the compressor control volume reduce to:

$$\dot{I}_{compressor} = -\dot{W}_{shaft} + \dot{m}(h_1 - h_2 - T_0(s_1 - s_2)), \quad (12)$$

where the sign of $\dot{W}_{shaft}$ is negative. When including the ambient in the control volume enclosing the intercooler, assuming that the temperature of the ambient medium receiving intercooler heat eventually converges to T_0, the exergy balance can be expressed as:

$$\dot{I}_{intercooler} = \dot{m}(h_2 - h_3 - T_0(s_2 - s_3)) \quad (13)$$

This is the expression for total intercooler irreversibilities. This can be further decomposed into respective losses caused by heat rejection and pressure drop through the heat exchanger, with the latter component obtainable from Eq. (7).

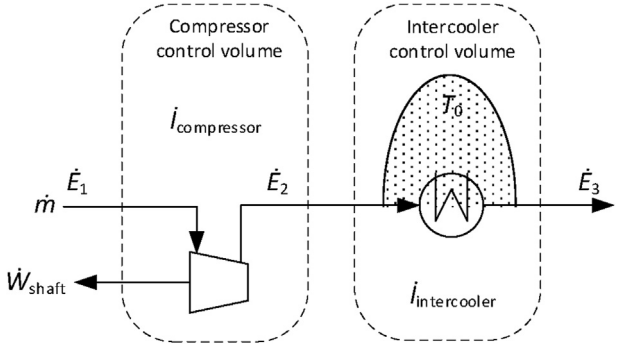

Fig. 4 – Exergy balance for an adiabatic compressor and subsequent cooling stage.

Cryo-expanders

The function of the cryo-expanders in the liquefier is to induce temperature drops by lowering the enthalpy of the hydrogen streams by expansion. For an adiabatic expansion from inlet State 1 to the outlet State 2, the exergy balance for a cryo-expander can be expressed as:

$$\dot{I}_{expander} = \dot{m}(-T_0(s_1 - s_2)) \quad (14)$$

An additional potential function of the cryo-expanders, however not exploited in state-of-the-art liquefiers, is to recover shaft power to reduce the net power requirement of liquefaction. In the current process, however, it is assumed that the expanders are coupled with brakes, so that the power is eventually dissipated by a coolant on the brake-side of the shaft and rejected as heat to the ambient. Hence, the total irreversibility for the cryo-expander, including the brake, becomes:

$$\dot{I}_{expander+brake} = \dot{m}(h_1 - h_2 - T_0(s_1 - s_2)) \quad (15)$$

Isenthalpic devices and processes

Like for compressors and expanders, devices such as ejectors and valves are assumed to be adiabatic and thus isenthalpic.

Control valves and throttling valves

The exergy balance of adiabatic valves gives the following expression for the irreversibility:

$$\dot{I}_{valve} = \dot{m}(-T_0(s_1 - s_2)) \quad (16)$$

Ejector for boiloff gas recompression

In the ejector, the high-pressure motive stream is accelerated and expanded through the motive nozzle to a static pressure level lower than that of the boiloff gas, inducing entrainment of the latter stream from the suction nozzle. Upon mixing, the aggregate stream is compressed in a diffusor and discharged. An illustration of the ejector arrangement is shown in Fig. 5, and the exergy balance for an adiabatic unit is expressed as:

$$\dot{I}_{ejector} = \dot{m}_1(h_1 - T_0 s_1) + \dot{m}_2(h_2 - T_0 s_2) - \left(\dot{m}_1 + \dot{m}_2\right)(h_3 - T_0 s_3) \quad (17)$$

Results

In the following, a detailed analysis of the useful exergy transfer and irreversibilities will be presented on a component level, which facilitates an in-depth discussion on how to

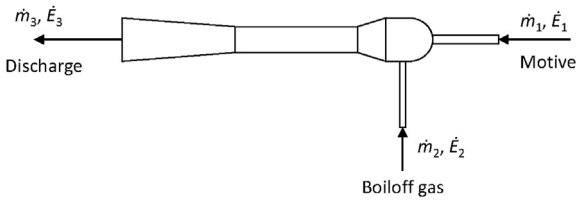

Fig. 5 – Ejector arrangement with motive, suction and discharge streams.

rationally increase the energy efficiency. All exergy figures are scaled with the hydrogen feed flowrate such that the unit displayed is kilowatt-hours per kg hydrogen feed.

Mixed-refrigerant pre-cooling cycle

Pre-cooling of the hydrogen feed from ambient temperature down to 114 K is provided solely by the mixed-refrigerant cycle in the present liquefier configuration, which allows the stand-alone exergy efficiency of the control volume encompassing this sub-process to be calculated. The net exergy input to the mixed refrigerant pre-cooling cycle equals the shaft power of the two compressors stages and the liquid pump pressurising the condensed components after the first intercooler stage. The total specific power input is 0.786 kWh/kg_{feed}, 0.334 kWh/kg_{feed} of which is converted to useful exergy output, equivalent to the exergy added to the hydrogen in HX-1. The overall exergy efficiency of the pre-cooling process is therefore 42.5%. Correspondingly, the total specific irreversibility in the pre-cooling process is 0.452 kWh/kg_{feed} and is allocated in different parts of the process, as shown in Fig. 6. As a control of the calculations of individual irreversibility rates and exergy conversion, the sum of exergy input and sum of power input were found to match exactly, as can be observed in Fig. 6. The relative error margin between the independently calculated results on left- and right-hand side is $8 \cdot 10^{-7}$, which acts as a check of correct use of the methodology. It also shows that chemical exergy must be accounted for to obtain correct exergy balance results, as stressed in the Background and motivation section above.

The single largest exergy loss of about 0.137 kWh/kg_{feed}, occurs inside HX-1 due to finite temperature differences between the hot-side and cold-side streams (0.116 kWh/kg_{feed}) as well as pressure losses (0.022 kWh/kg_{feed}) through the heat exchanger. The first- and second-stage compressor intercoolers cause losses equivalent to 0.077 kWh/kg_{feed} and 0.087 kWh/kg_{feed}, respectively. Despite a lower mass flowrate through the second-stage cooler compared to the first stage, and virtually equal compressor discharge temperatures, the second-stage heat duty and exergy losses are still higher due to increased condensation heat. The compressor irreversibilities are found to be 0.056 kWh/kg_{feed} and 0.038 kWh/kg_{feed} for the first and second stage. J–T throttling of the mixed refrigerant in the cold end of the process causes irreversibilities equivalent to 0.052 kWh/kg_{feed}. The remainder of the losses are distributed between irreversibilities from gas-liquid mixing (0.004 kWh/kg_{feed}) and in the pump (0.001 kWh/kg_{feed}), which are the least prominent drivers of exergy losses in the pre-cooling cycle.

Hydrogen Claude cycle

From the inlet of HX-3, downstream of the adiabatic ortho-para conversion bed, cooling of the hydrogen feed stream from 117.9 K to subcooled liquid at the outlet of HX-7 is provided by the hydrogen Claude cycle. In addition to raising the exergy level of the hydrogen feed between these thermodynamic states, calculated to 2.34 kWh/kg_{feed}, exergy is also transferred to the re-liquefied boiloff gas through ejector recompression and subsequent condensation and

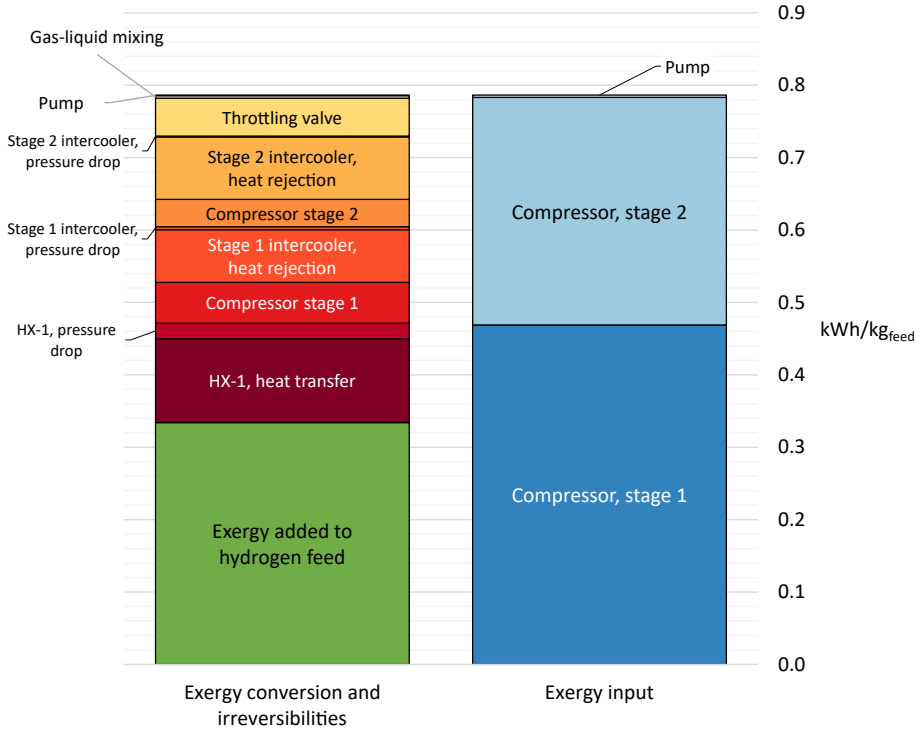

Fig. 6 – Exergy balance of the mixed-refrigerant pre-cooling cycle, where the exergy losses and the exergy added to the hydrogen feed balance the power input of the pump and the compressors.

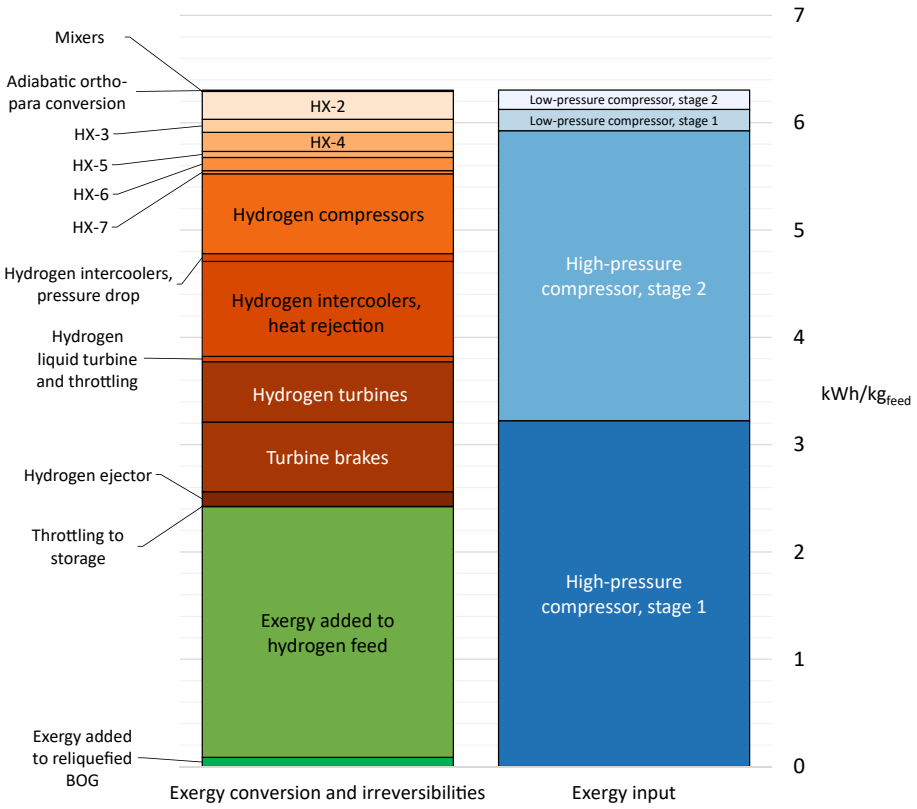

Fig. 7 – Exergy balance for the Claude cycle, where the exergy losses and the exergy added to the hydrogen feed balance the power input of the compressors.

subcooling in HX-7. The magnitude of this exergy transfer is 1.50 kWh/kg_{BOG}, and correspondingly 0.085 kWh/kg_{feed} when scaled with the hydrogen feed rate (125 t/d). Fig. 7 shows the stand-alone exergy balance of the hydrogen Claude cycle.

The net exergy input to the Claude cycle is the compressor power of the low- and high-pressure hydrogen compressors LPC-1, LPC-2, HPC-1 and HPC-2, which sums to 6.30 kWh/kg_{feed}. This exergy input is converted to 2.42 kWh/kg of useful output, which corresponds to an exergy efficiency of 38.4%. This is significantly lower than that of the mixed-refrigerant pre-cooling cycle for different reasons. It is important to note that the current exergy balance and efficiency calculation assumes that the shaft power generated by the turbines is fully dissipated. For the capacity of the liquefier in consideration, losses can be reduced considerably by replacing the turbine brakes with electric generators, the potential of which is discussed in a subsequent section.

The largest shares of irreversibilities are found in the hydrogen compressor train, split into compressor irreversibilities (0.74 kWh/kg_{feed}) and intercooler irreversibilities (0.96 kWh/kg_{feed}). Intercooler irreversibilities are attributed to heat rejection (0.89 kWh/kg_{feed}) and pressure drop (0.07 kWh/kg_{feed}). Second to the compressor train are irreversibilities in the cryogenic hydrogen turbines (0.56 kWh/kg_{feed}) and the brakes dissipating the shaft power (0.65 kWh/kg_{feed}). The total irreversibility rate in heat exchangers HX-2 through HX-7 is 0.77 kWh/kg_{feed}. The isenthalpic ejector process, where the hydrogen feed is throttled from high pressure and boiloff gas from the LH_2 storage is recompressed, accounts for an irreversibility rate of 0.14 kWh/kg_{feed}. As can be further observed, mixing of hydrogen streams (0.004 kWh/kg_{feed}), adiabatic ortho-para conversion upstream HX-3 (0.007 kWh/kg_{feed}) and throttling losses to LH_2 storage (0.002 kWh/kg_{feed}) are only minor causes of irreversibilities. As shown in Fig. 7, the sum of all individually calculated component irreversibilities and exergy conversions matches the sum of compressor power input, with a relative error margin of $2 \cdot 10^{-4}$, which acts as a self-check of the calculations for the hydrogen Claude cycle.

Heat exchangers

For all cryogenic heat exchangers in the Claude cycle as well as HX-1 in the pre-cooling process, a decomposition of irreversibilities caused by finite-temperature heat transfer and pressure loss is shown in Fig. 8.

As explained in the description of the process, the simulations assume equilibrium conversion of ortho-hydrogen to para-hydrogen in the catalyst-filled channels. Hence, a consequence of this is zero losses due to non-equilibrium ortho-para conversion, which renders heat transfer irreversibilities and throttling irreversibilities the only exergy losses. In order to illustrate the additional losses that can be expected to occur due to non-equilibrium conversion, the results from this work are compared to results recently presented by Skaugen et al. [29]. Skaugen et al. used detailed mathematical

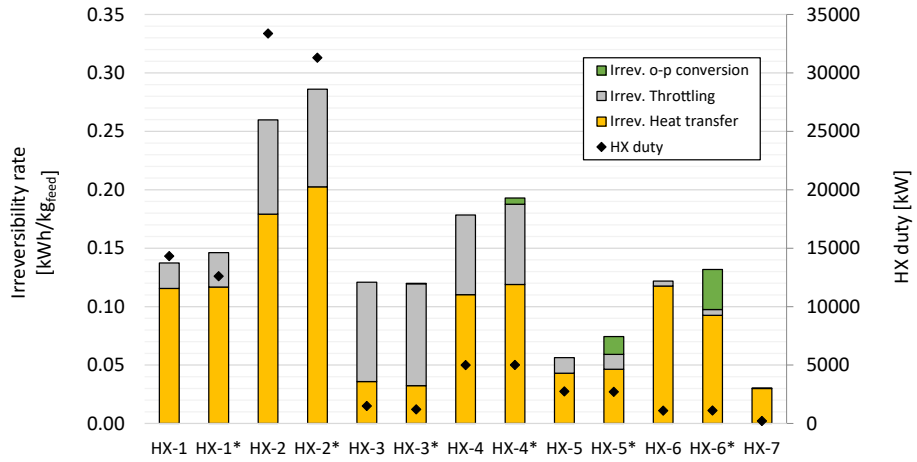

Fig. 8 – Heat exchanger irreversibilities decomposed into losses caused by finite-temperature heat transfer and pressure drop. Irreversibility rates are scaled by the net output of hydrogen, (125 t/d). Titles with asterisks (*) represent results by Skaugen et al. [29].

models of the plate-fin heat exchangers, including the kinetics of the catalysed ortho-para conversion.

As can be observed, the results from detailed heat exchanger simulations [29] and the current simplified heat exchanger models agree to a large extent. Some discrepancies can be observed, which are partly due to slightly different conditions of the inlet streams, particularly in HX-1 and HX-2, where the hot-stream inlet temperatures are 10 K higher. For HX-3 through HX-6, the comparisons are more consistent. The pressure drop calculated for each process stream in Ref. [29] were adopted in this work. For HX-6, for instance, the irreversibilities caused by pressure losses are therefore close to identical, while those caused by heat transfer differ visibly. The main explanation of the discrepancy is that since the present model assumes continuous ortho-para conversion in equilibrium, the heat duty and thus the effective heat capacity of the hydrogen feed stream is higher in the ideal case than for the detailed simulations, where the conversion rate and thus effective heat capacity is lower. As a result, the temperature differences and resulting irreversibility rate caused by heat transfer becomes higher in the ideal case. The losses occurring due to non-equilibrium conversion will in practice materialise in the form of increased refrigeration duty in the condensing and subcooling process taking place in HX-7. When converting residual fractions of ortho-hydrogen to the desired LH_2 product specification (in this work assumed to be 97% para-hydrogen) in catalyst-filled heat exchanger channels, the exothermic reaction increases the duty and thus also the evaporation rate of low-pressure hydrogen on the cold side. This propagates in the form of increased throughput in compressors LPC-1 and LPC-2, as well as HPC-1 and HPC-2, which in turn increases the power requirement. As long as the ortho-para conversion does not lag too far behind the equilibrium composition, like for instance in HX-3, there is a good agreement between the irreversibility rates from the heat exchangers represented in this work, simulated by use of "equilibrium hydrogen" that effectively incorporates the heat of reactions into and effective heat capacity [28], and a nonequilibrium treatment by detailed modelling from the work by Skaugen et al. [29]. Despite that "equilibrium hydrogen" has received some critique in recent literature [34], this clearly demonstrates the usefulness of the concept in an effective treatment of the heat exchangers of a hydrogen liquefaction process. In Ref. [29,35], it was shown that there is significant potential to reduce the irreversibilities in heat exchangers by improved design and operation. We refer to these works for further details on how to improve the performance of the heat exchangers and will in the following outline additional measures to improve the efficiency.

Overall exergy balance and irreversibilities

Irreversibilities in the liquefaction process are grouped and ranked category-wise in the bar diagram shown in Fig. 9. Also shown on the right-hand vertical axis is the cumulative irreversibility rate starting with the largest group. Under the current categorisation and bundling of irreversibilities, hydrogen compressor intercoolers make the single largest contribution to irreversibilities with 0.96 kWh/kg$_{feed}$. Cryogenic heat exchangers HX-1 through HX-7 make the second largest group with 0.91 kWh/kg$_{feed}$ in total. The losses in the hydrogen compressors make the third largest contribution, followed by losses from turbine brakes and thereafter from losses in the cryogenic hydrogen turbines. The overall exergy balance of the liquefaction process is summarised in Table 2, where the results derived from the detailed bottom-up approach are compared to those derived from the top-down exergy balance. The top-down results are shown on the right-hand column through the power input for hydrogen and mixed-refrigerant compression obtained from the liquefier simulation model, which sum to 7.09 kWh/kg when scaled with the hydrogen feed rate. The indicator that reveals to what extent the detailed bottom-up exergy analysis for all process components and sub-systems has provided correct results, is to compare the sum of all irreversibilities and useful exergy output with the total power input. The bottom-up

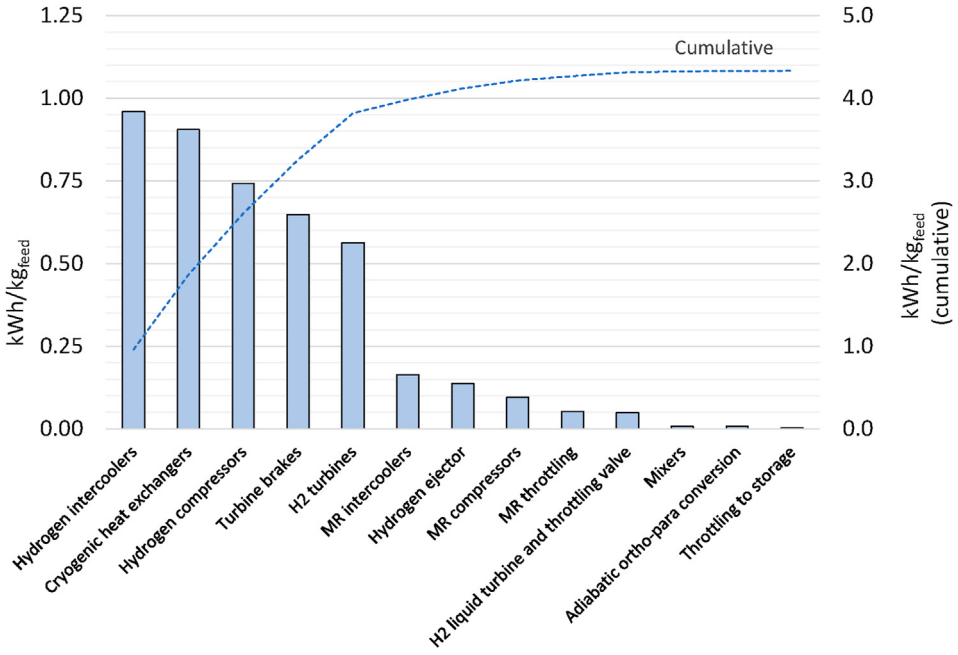

Fig. 9 – Irreversibilities by component category, scaled by hydrogen feed rate (125 t/d).

results are shown in the left-hand column and include all identified and individually calculated irreversibilities as well as useful exergy output transferred to the hydrogen feed and to the re-liquefied boiloff gas. Total irreversibilities, 4.332 kWh/kg_{feed}, and total useful exergy output, 2.757 kWh/kg_{feed}, makes a total of 7.089 kWh/kg_{feed}. The relative error between the two independently calculated exergy numbers is approximately $2 \cdot 10^{-4}$.

With reference to our statement in the introduction about the problem with ignoring pressure losses, which has been

Table 2 – Overall exergy balance of the liquefaction process. Units for all numbers are scaled with the hydrogen feed rate (125 t/d), to kWh per kg hydrogen feed.

	Category	Exergy conversion (bottom-up)		Exergy input (top-down)	
Irreversibilities/Exergy losses	Hydrogen intercoolers, heat rejection	0.886			
	Hydrogen compressors	0.742			
	Turbine brakes	0.648			
	Cryogenic heat exchangers, heat transfer	0.633			
	Hydrogen turbines	0.563			
	Cryogenic heat exchangers, pressure drop	0.273			
	MR intercoolers, heat rejection	0.159			
	Hydrogen ejector	0.137			
	MR compressors	0.095			
	Hydrogen intercoolers, pressure drop	0.073			
	MR throttling	0.052			
	H_2 liquid turbine and throttling valve	0.049			
	Mixers	0.008			
	Adiabatic ortho-para conversion	0.007			
	MR intercoolers, pressure drop	0.005			
	Throttling to storage	0.002			
Useful exergy output	Exergy added to hydrogen feed		2.671		
	Exergy added to re-liquefied boiloff gas		0.085		
Exergy input	Hydrogen compressors power				6.304
	MR compressors and pump power				0.786
Sum		4.332	2.757		7.090
Total exergy balance (checksum)		**7.089**			**7.090**

done in several works, the irreversibilities attributed to pressure losses in heat exchangers and intercoolers amount to 0.35 kWh/kg_{feed}, which corresponds to about 8% of all irreversibilities.

Measures for reducing exergy losses and improving efficiency

Several options exist for improving the efficiency by reducing exergy losses in the liquefaction cycle, and some of the most interesting will be discussed in the following. The techno-economic attractiveness and viability of each measure on different scales will not be analysed in further detail and represents future work.

Power recovery from the shafts of the hydrogen turbines is arguably the most obvious means for reducing the irreversibility rate and thus the net power requirement of the liquefaction cycle. As shown in Table 2, the specific irreversibility rate from turbine brakes is about 0.65 kWh/kg_{feed}. The recoverable power will depend on the overall shaft-to-power efficiency when coupling the turbines inside the coldbox with electric generators. According to Refs. [15], 80% mechanical to electrical energy recovery is on the conservative side for hydrogen turbines. If as much as 80% of the shaft power can be recovered (shaft-to-shaft via an electric generator and drive) and used for compression, the specific hydrogen liquefaction power can be reduced by about 7%, from 7.09 kWh/kg to 6.57 kWh/kg. This corresponds to about 22.5 GWh of annual savings in power demand for the 125 t/d plant, assuming 95% plant availability.

The mixed-refrigerant pre-cooling cycle accounts for only 10.4% of the total irreversibilities and 11.1% of the power requirement in the liquefier. With respect to measures for improving the liquefier efficiency, these numbers can be somewhat deceptive and underestimate the improvement potential. Better tailored mixed-refrigerant cycles can provide considerably deeper pre-cooling, potentially down to around 80 K, while maintaining clog-free operation by avoiding freeze-out in the cold end [36]. More advanced cycle configurations, such as dual mixed-refrigerant cascade cycles or auto-cascade cycles, give a higher degree of freedom for tailoring the chemical compositions, the refrigerant flowrates and the high- and low-pressure levels, in order to cater to the thermal duties allocated at different temperature levels. The realisation of deeper pre-cooling beyond what the already proven refrigerants and process configurations from LNG technology can provide, will require further maturation and qualification to ensure reliable, clog-free and safe operation.

Irreversibilities due to cold-side throttling in the mixed-refrigerant cycle can be reduced by replacing the throttling valve fully by a liquid expander, or partly through a serial configuration. Reducing the portion of isenthalpic expansion and instead lowering the enthalpy of the expanded stream, will reduce the entropy production and thus also irreversibilities. This will enable reduced high-/low-pressure ratio as well as reduced refrigerant flowrate [13], in turn reducing compressor duties.

By extending the temperature range of the mixed-refrigerant pre-cooling cycle, it can offset a considerable duty otherwise provided by the generally less exergy-efficient hydrogen Claude cycle. Thus, lowering the pre-cooling temperature threshold will also reduce the total irreversibility rate attributed to hydrogen compressors, intercoolers, turbines and other process units in the Claude cycle, since its duty in the upper temperature intervals of this cycle is reduced.

The ejector that throttles the pre-cooled hydrogen feed and recompresses the boiloff gas from the LH_2 storage accounts for 0.14 kWh/kg of irreversibilities, that is, 3% of the total. It is likely that ejector recompression of the boiloff gas can be achieved with lower pressure drop across the device. This can enable the use of a dense-phase/liquid expander in series with an ejector, which in turn will contribute to reducing entropy production and irreversibilities. As a result, the discharged two-phase hydrogen stream will have a lower vapour fraction, which in turn reduces the duty in the flooded evaporator HX-7. This is an example of potential "propagation effects" of efficiency measures. The lowered HX-7 duty reduces mass flowrates through the low- and high-pressure compressors as well as their intercoolers, which in turn reduces the irreversibilities caused by compression and intercooler heat rejection.

To a certain extent, thermodynamic losses can be categorised as either "unavoidable" and "avoidable" irreversibilities. As exemplified by the propagation effects as described above, these categories cannot always be unambiguously distinguished since they can be directly and indirectly interdependent. In the current configuration, however, the dissipated shaft power generated by the cryo-expanders is an obvious example of a highly "avoidable" portion of irreversibility.

The introduction of high-temperature chillers to supplement ambient cooling could be considered as part of more advanced pre-cooling process designs. High-temperature chillers can operate with a high coefficient of performance (COP) and can contribute to avoiding potentially narrow temperature approaches in the hot end of both the pre-cooling process as well as in the recuperative hydrogen pre-cooling heat exchanger HX-2. Moreover, chillers can be used to lower the temperature and volume flow in the compressors, thereby reducing their gross power demand. According to Ohlig and Decker [22], a 6% reduction in energy demand can be realised at the expense of 3% higher investments.

Another potential means for power recovery in the process can be identified in the waste heat from the intercoolers, which is one of the major causes of irreversibilities. This is particularly parasitic for the hydrogen intercoolers, where the hot-side inlet temperatures are around 100 °C. Power recovery from waste heat can be achieved by Rankine cycles, which is an option applicable to many cases of industrial waste heat utilisation [37]. The economic viability of such heat-to-power applications depends on several factors related to power cost and investment cost.

In addition to the above-mentioned improvement opportunities, improvements in compressor and expander efficiency, particularly in the Claude cycle, can have a high impact on the overall liquefier efficiency. Further measures that can become more viable with increasing scale are for instance the use of two-stage hydrogen expansion and condensation/subcooling, as well as other more advanced process configurations in the cold end of the liquefaction process.

In addition to the improvement potential for existing technologies, novel solutions in the mid-to long-term, such as those briefly reviewed in the Background section, could lead to significant reduction of the exergy losses. Cryogenic refrigerants such as helium/neon/hydrogen mixtures [38–40], can give sufficiently high molecular mass to allow the practical use of centrifugal compressors, which can realise a favourable cost-scaling exponent compared to reciprocal piston compressors. This, and the potential for higher compressor efficiency, can be elements of high importance when considering substantial and unprecedented scaling-up of liquefaction plants. However, the procurement and maintenance cost of the centrifugal compressors must be compared to the extra cost of the cryogenic refrigerant coming both from the initial investment as well as for compensating for refrigerant lost through leaks and the additional sealing required to minimise the occurrence of leaks. A largely unexplored topic is to tailor-make cryogenic mixed refrigerants to achieve a tight thermal match also in the bottom part of the hydrogen liquefaction process. Further analysis of this falls beyond the scope of the present work.

Conclusions

The difference between the exergy input and useful exergy output is equal to the sum of exergy destruction, or irreversibilities, occurring in a process. In order to understand where and in what magnitude the different losses occur in a hydrogen liquefier, irreversibilities of a simulation model representing a large-scale hydrogen liquefier with 7.09 kWh/kg_{feed} power requirement have been decomposed to the single-component level. An overview of the causes of irreversibilities was obtained and discussed in detail. For the Claude hydrogen liquefier with mixed-refrigerant pre-cooling, the main losses are caused by the Claude cycle, which cools the hydrogen from 117.9 K to its final liquid-product state and also re-liquefies boiloff gas from the liquid hydrogen storage. In the Claude cycle, approximately 90% of the total irreversibilities can be identified. In comparison, the mixed-refrigerant cycle cooling hydrogen from the feed temperature to 114 K is responsible for only 10% of the total irreversibilities. The largest losses are identified in the hydrogen compressor train in the Claude cycle, with compressors and intercoolers causing 39% of total losses. By comparing to detailed heat exchanger simulations, it was shown that the "equilibrium hydrogen" thermodynamic description gave a reliable representation of the effective exergy destruction in the heat exchangers, provided that the pressure drop was taken into account. The cryogenic heat exchangers account for 21% of the total losses. While irreversibilities caused by the hydrogen turbines constitute 13% of the total, the corresponding number for irreversibilities caused by turbine brakes is 15%. An 80% shaft-to-shaft power recovery would reduce the specific power requirement to 6.57 kWh/kg_{feed}. The impact of improving the pre-cooling cycle can be significant since cascade processes can lower the pre-cooling temperature considerably and such shift a considerable portion of refrigeration duty from the less exergy-efficient Claude cycle over to the more efficient pre-cooling cycle.

In the work on identifying further rational process improvements, several measures and modifications are possible, many of which are possible to implement simultaneously while others are mutually exclusive. Examples of further options are: Liquid expander in series with the ejector, chillers to supplement ambient intercooling, two-stage hydrogen expansion and condensation, intercooler waste heat-to-power. The viability of each measure or combination of measures depends on the trade-off between on the one hand increased capital and complexity-driven expenditures and on the other, reduced energy expenditures. High capacity will shift the cost weighting towards operational expenditures and if specific capital expenditures become more favourable with scale, efficiency-improving measures will generally become increasingly attractive.

For substantial scaling-up in the long term, novel technologies are promising. An example of this is cycles with new cryogenic refrigerant mixtures of helium/neon/hydrogen enabling the use of centrifugal compressors, which are generally well suited and scalable to very high capacities.

Declaration of competing interest

The authors declare that they have no known competing financial interests or personal relationships that could have appeared to influence the work reported in this paper.

Acknowledgements

This publication is based on results from the research project Hyper, performed under the ENERGIX programme. The authors acknowledge the following parties for financial support: Equinor, Shell, Kawasaki Heavy Industries, Linde Kryotechnik, Mitsubishi Corporation, Nel Hydrogen, Gassco and the Research Council of Norway (255107/E20).

REFERENCES

[1] Valenti G. Hydrogen liquefaction and liquid hydrogen storage. In: Gupta RB, Basile A, Veziroğlu TN, editors. Compendium of hydrogen energy volume 2: hydrogen storage, transportation and infrastructure. vol. 2. Woodhead Publishing; 2016. p. 27–51.

[2] Norled. Partners receive PILOT-E support to develop liquid hydrogen supply chain for maritime applications in Norway. 16 December 2019. Retrieved from: https://www.norled.no/en/news/partners-receive-pilot-e-support-to-develop-liquid-hydrogen-supply-chain-for-maritime-applications-in-norway/.

[3] Andersson J, Grönkvist S. Large-scale storage of hydrogen. Int J Hydrogen Energy 2019;44(23):11901–19.

[4] LNG Fundamentals. In: Mokhatab S, Mak JY, Valappil JV, Wood DA, editors. Handbook of liquefied natural gas. vol. 1. Gulf Professional Publishing; 2014. p. 1–106.

[5] IEA. The future of hydrogen. Seizing today's opportunities. Technical report. International Energy Agency; 2019.

[6] Kamiya S, Nishimura M, Harada E. Study on introduction of CO_2 free energy to Japan with liquid hydrogen. Phys Proc 2015;67:11–9.
[7] Bracha M, Lorenz G, Patzelt A, Wanner M. Large-scale hydrogen liquefaction in Germany. Int J Hydrogen Energy 1994;19(1):53–9.
[8] Cardella U, Decker L, Klein H. Roadmap to economically viable hydrogen liquefaction. Int J Hydrogen Energy 2017;42(19):13329–38.
[9] Heiersted RS, Lillesund S, Nordhasli S, Owren G, Tangvik K. The snohvit design reflects a sustainable environmental strategy. In: Proceedings – LNG 14, the 14th international conference & exhibition on liquefied natural gas, Doha, Qatar; March, 2004. p. 21–4. PS5-4.
[10] Valenti G, Macchi E. Proposal of an innovative, high-efficiency, large-scale hydrogen liquefier. Int J Hydrogen Energy 2008;33(12):3116–21.
[11] Quack H, et al. Selection of components for the IDEALHY preferred cycle for the large scale liquefaction of hydrogen. AIP Conference Proceedings 2014;1573:237–44. https://doi.org/10.1063/1.4860707.
[12] Stolzenburg K, et al. Efficient liquefaction of hydrogen: results of the IDEALHY project. 20th Energie-Symposium. Germany: Stralsund; 7–9 November 2013. Retrieved from: https://www.idealhy.eu/uploads/documents/IDEALHY_XX_Energie-Symposium_2013_web.pdf.
[13] Berstad D, Stang JH, Nekså P. Large-scale hydrogen liquefier utilising mixed-refrigerant pre-cooling. Int J Hydrogen Energy 2010;35(10):4512–23.
[14] Quack H. Conceptual design of a high efficiency large capacity hydrogen liquefier. Adv Cryog Eng 2001;47:255–63.
[15] Cardella U, Decker L, Sundberg J, Klein H. Process optimization for large-scale hydrogen liquefaction. Int J Hydrogen Energy 2017;42(17):12339–54.
[16] Krasae-in S, Stang JH, Nekså P. Simulation on a proposed large-scale liquid hydrogen plant using a multi-component refrigerant refrigeration system. Int J Hydrogen Energy 2010;35(22):12531–44.
[17] Asadnia M, Mehrpooya M. A novel hydrogen liquefaction process configuration with combined mixed refrigerant systems. Int J Hydrogen Energy 2017;42(238):15564–85.
[18] Lee H, Shao Y, Lee S, Roh G, Chun K, Kang H. Analysis and assessment of partial re-liquefaction system for liquefied hydrogen tankers using liquefied natural gas (LNG) and H_2 hybrid propulsion. Int J Hydrogen Energy 2019;44(29):15056–71.
[19] Yin L, Ju Y. Process optimization and analysis of a novel hydrogen liquefaction cycle. Int J Refrig 2020;110:219–30.
[20] Sadaghiani MS, Mehrpooya M. Introducing and energy analysis of a novel cryogenic hydrogen liquefaction process configuration. Int J Hydrogen Energy 2017;42(9):6033–50.
[21] Sadaghiani MS, Mehrpooya M, Ansarinasab H. Process development and exergy cost sensitivity analysis of a novel hydrogen liquefaction process. Int J Hydrogen Energy 2017;42(50):29797–819.
[22] Ohlig K, Decker L. The latest developments and outlook for hydrogen liquefaction technology. AIP Conference Proceedings 2014;1573:1311–7. https://doi.org/10.1063/1.4860858.
[23] Krasae-in S, Bredesen AM, Stang JH, Nekså P. Simulation and experiment of a hydrogen liquefaction test rig using a multi-component refrigerant refrigeration system. Int J Hydrogen Energy 2011;36(1):907–19.
[24] Bischoff S, Decker L. First operating results of a dynamic gas bearing turbine in an industrial hydrogen liquefier. AIP Conference Proceedings 2010;1218(1).
[25] Elbel S, Hrnjak P. Experimental validation of a prototype ejector designed to reduce throttling losses encountered in transcritical R744 system operation. Int J Refrig 2008;31(3):411–22.
[26] Leachman JW, Jacobsen RT, Penoncello SG, Lemmon EW. Fundamental equations of state for parahydrogen, normal hydrogen, and orthohydrogen. J Phys Chem Ref Data 2009;38(3):721–48.
[27] Lemmon EW, Huber ML, McLinden MO. REFPROP: reference fluid thermodynamic and transport properties, NIST standard reference database. National Institute of Standard and Technology, Gaithersburg, MD, USA.
[28] Valenti G, Macchi E, Brioschi S. The influence of the thermodynamic model of equilibrium-hydrogen on the simulation of its liquefaction. Int J Hydrogen Energy 2012;37(14):10779–88.
[29] Skaugen G, Berstad D, Wilhelmsen Ø. Evaluating the potentials of catalyst-filled plate-fin and spiral-wound heat exchangers in a large-scale Claude hydrogen liquefaction process. Int J Hydrogen Energy 2020;45(11):6663–79.
[30] Kotas TJ. The exergy method of thermal plant analysis. Melbourne, FL, USA: Krieger Publishing Company; 1995. reprinted.
[31] Berstad D, Stang JH, Nekså P. Comparison criteria for large-scale hydrogen liquefaction processes. Int J Hydrogen Energy 2009;34(3):1560–8.
[32] Kvalsvik KH, Berstad D, Wilhelmsen Ø. Dynamic modelling of a liquid hydrogen loading cycle from onshore storage to a seaborne tanker. In: Proceedings of the 15th IIR international conference: prague, Czech republic, april 8–11, 2019; 2019. https://doi.org/10.18462/iir.cryo.2019.0019. Cryogenics.
[33] Wilhelmsen Ø, Berstad D, Aasen A, Nekså P, Skaugen G. Reducing the exergy destruction in the cryogenic heat exchangers of hydrogen liquefaction processes. Int J Hydrogen Energy 2018;10(8):5033–47.
[34] Lasala S, Privat R, Arpentinier P, Jaubert J-N. Note on the inconsistent definition assigned in the literature to the heat capacity of the so-called "equilibrium hydrogen" mixture. Fluid Phase Equil 2020;504:112325.
[35] Hånde R, Wilhelmsen Ø. Minimum entropy generation in a heat exchanger in the cryogenic part of the hydrogen liquefaction process: on the validity of equipartition and disappearance of the highway. Int J Hydrogen Energy 2019;44(29):15045–55.
[36] Cardella U, Decker L, Klein H. Low-temperature mixed-refrigerant for hydrogen precooling in large scale. Patent 2017. no. WO2017072221A1, https://patents.google.com/patent/WO2017072221A1/.
[37] Quoilin S, Van Den Broek M, Declaye S, Dewallef P, Lemort V. Techno-economic survey of organic rankine cycle (ORC) systems. Renew Sustain Energy Rev 2013;22:168–86.
[38] Aasen A, Hammer M, Ervik Å, Müller EA, Wilhelmsen Ø. Equation of state and force fields for Feynman–Hibbs-corrected Mie fluids. I. Application to pure helium, neon, hydrogen, and deuterium. J Chem Phys 2019;151:064508.
[39] Aasen A, Hammer M, Ervik Å, Müller EA, Wilhelmsen Ø. Equation of state and force fields for Feynman–Hibbs-corrected Mie fluids. II. Application to mixtures of helium, neon, hydrogen, and deuterium. J Chem Phys 2020;152:074507.
[40] Aasen A, Hammer M, Lasala S, Jaubert J-N, Wilhelmsen Ø. Accurate quantum-corrected cubic equations of state for helium, neon, hydrogen, deuterium and their mixtures. Fluid Phase Equil 2020;524:112790.